Journal of Structural Geology 30 (2008) 976–992

Contents lists available at ScienceDirect

Journal of Structural Geology

journal homepage: www.elsevier.com/locate/jsg

Omphacite textures in eclogites of the Tauern Window: Implications for the exhumation of the Eclogite Zone, Eastern Alps

K. Neufeld [a,*], U. Ring [b], F. Heidelbach [c], S. Dietrich [a], R.D. Neuser [d]

[a] Institut für Geowissenschaften, Universität Mainz, Becherweg 21, 50099 Mainz, Germany
[b] Department of Geological Sciences, University of Canterbury, Private Bag 4800, Christchurch, New Zealand
[c] Bayerisches Geoinstitut, Universität Bayreuth, 95440 Bayreuth, Germany
[d] Zentrales Rasterelektronenmikroskop, Ruhr-Universität Bochum, Universitätstrasse 150, 44801 Bochum, Germany

ARTICLE INFO

Article history:
Received 27 October 2007
Received in revised form 7 March 2008
Accepted 29 March 2008
Available online 9 April 2008

Keywords:
Omphacite
Lattice preferred orientation
Eclogite Zone
Exhumation
Extrusion wedge

ABSTRACT

We discuss the relationship of omphacite lattice preferred orientation (LPO) patterns in eclogite and kinematic indicators in the matrix surrounding the eclogite during the very rapid exhumation of the deeply buried Eclogite Zone in the Tauern Window of the Eastern Alps. LPO patterns are presented from profiles parallel to the eclogite stretching lineation across the Eclogite Zone. The omphacite textures show symmetric patterns across the entire Eclogite Zone; only in few cases slight asymmetries are observed. The patterns are characterized by an alignment of {110} with the foliation and a maximum of ⟨001⟩ close to the lineation and are indicative of deformation by intracrystalline glide on the (010) [001] and (110) [001] slip systems. The patterns have close resemblance to S-type LPO patterns and probably developed during the burial and accretion of the eclogites. We argue that the LPO patterns are not related to deformation associated with the very rapid exhumation of the Eclogite Zone. We conclude that exhumation-related deformation was concentrated in the metasedimentary rocks that surround the eclogites, allowing the eclogites to preserve their burial LPO signature during the exhumation process. Kinematic indicators show top-N thrusting at the base of the Eclogite Zone and sinistral strike-slip faulting at the top. Most of the kinematic indicators record blueschist- and greenschist-facies metamorphic conditions. However, because of the very rapid exhumation of the Eclogite Zone with rates exceeding 36 km Myr^{-1}, the kinematic indicators are interpreted to reflect the entire exhumation process from eclogite-facies conditions. We discuss a model according to which the Eclogite Zone was exhumed in an oblique extrusion wedge.

1. Introduction

The exhumation of extremely dense eclogites from great depths to mid-crustal levels is a fundamental problem in tectonics. Eclogites have a density of up to 3600 kg m^{-3} and are thus much denser than any other crustal rocks and also significantly denser than lithospheric mantle rocks (e.g. Ring et al., 1999). The deeply exhumed Eclogite Zone in the Tauern Window of the Eastern Alps is a superb example for addressing this problem because of the excellent preservation and exposure of eclogites.

The currently most favoured model for the exhumation of the Eclogite Zone with its eclogites and surrounding schists is that of wedge extrusion in a subduction channel (Kurz et al., 1998; Kurz and Froitzheim, 2002). Accordingly, the base of the Eclogite Zone is considered a top-N thrust and the top of the Eclogite Zone a top-S normal shear zone. We present a systematic study of lattice preferred orientation (LPO) patterns of omphacite from 20 eclogite samples taken along profiles parallel to the tectonic transport direction in the Eclogite Zone in order to see whether the proposed switch from top-N thrusting at the base to top-S normal shearing at the top of the Eclogite Zone is represented in the LPO patterns from a representative sample set. Furthermore, we present kinematic indicators from the Eclogite Zone especially from the contacts between the Eclogite Zone and its under- and overlying nappes. The combination of structural and textural data is then integrated into a tectonic model for the exhumation of the Eclogite Zone.

2. Geological setting

The Alps can be subdivided into the European continental sequences represented by the Helvetic Nappes at the base, overlying oceanic sequences of the Pennine Nappes and continental rocks of the Adriatic plate (Austroalpine and Southernalpine units) at the top (Fig. 1) (Selverstone, 1988; Ring et al., 1988; Schmid et al., 2004).

* Corrresponding author. Tel.: +49 613 1392 4368; fax: +49 613 1392 4769.
E-mail address: kneufeld@uni-mainz.de (K. Neufeld).

0191-8141/$ – see front matter © 2008 Elsevier Ltd. All rights reserved.
doi:10.1016/j.jsg.2008.03.010

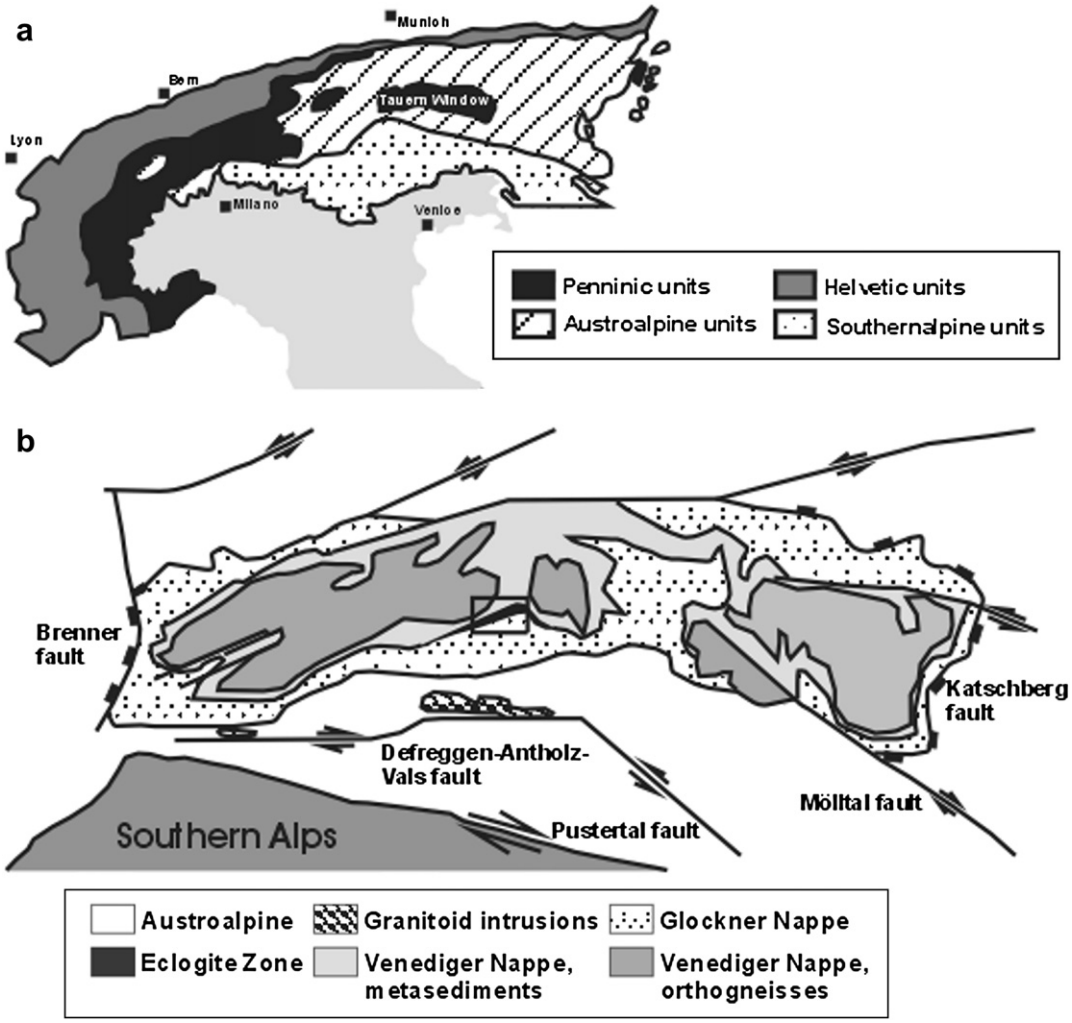

Fig. 1. The Tauern Window within the Alps (a) and location of the Eclogite Zone in the south-central Tauern Window of the Eastern Alps (b). The study area (central part of the Eclogite Zone) is marked by a box.

The Eastern Alps are dominated by the Austroalpine Nappes. In the Tauern and Engadin Windows the underlying rocks of the Pennine and Helvetic Nappes crop out (Frank et al., 1987).

From top to bottom the Tauern Window consists of the Penninic Glockner Nappe, the Eclogite Zone and the Venediger Nappe (Schmid et al., 2004). The Eclogite Zone forms a steeply S-dipping thrust sheet and consists of eclogite-facies metasediments with intercalated mafic igneous rocks. It is interpreted as a distal succession of the passive European continental margin (Helvetic Nappes) and is tectonically sandwiched between nappes of lower metamorphic grades. The Glockner Nappe is made up by rocks of oceanic affinity which reached blueschist-facies metamorphism (~8 kbar and 500 °C, Selverstone, 1993). The Venediger Nappe below the Eclogite Zone comprises gneisses and parautochthonous metasediments of the European margin. The rocks of the Venediger Nappe reached ~11 kbar and 540 °C (Selverstone, 1993). Recent studies show that the Tauern Window resulted from NNE-directed transpressive shortening (Rosenberg et al., 2004, 2007; Schmid et al., 2004).

The Eclogite Zone crops out along a strike length of 20 km. The north–south extent varies between 1.5 and 3 km. In the Eclogite Zone, eclogites occur as lenses with a maximum size of 1500 m by 700 m and a thickness of up to 300 m (Figs. 2 and 3). Most of the eclogite blocks are significantly smaller with a common size of about 100 m by 20 m. The eclogite blocks are embedded in a matrix of lower density rocks, i.e. garnet mica schist, calc schist, quartzite and marble. Our detailed field work showed that eclogite lenses make up ~30% of the Eclogite Zone. The eclogite lenses are not pure eclogite but are rather intermixed eclogite and mica schist.

Peak metamorphism in the Eclogite Zone occurred at ~25 kbar and ~650 °C and affected the eclogite blocks and the surrounding matrix in a coherent fashion (Holland, 1977; Frank et al., 1987; Stöckhert et al., 1997; Hoschek, 2007). Hoschek (2007) showed that the PT path has a clockwise shape and Glodny et al. (2005, in press) dated the peak of eclogite-facies metamorphism at 31 Ma.

3. Previous work

3.1. Eclogite zone

England and Holland (1979) argued that very fast exhumation allowed the dense eclogite blocks to overcome their negative buoyancy and to rise up within their mica-schist matrix. They envisaged that lenses of dense eclogite were transported in an uprising lower density matrix and showed that this mechanism can only work when exhumation rates are >40 km Myr^{-1}. Recently, Glodny et al. (2005) showed that minimum exhumation rates in the Eclogite Zone are 36 km Myr^{-1} and thus indeed of the order which England and Holland predicted. Behrmann and Ratschbacher (1989) argued that vertical thinning due to overall coaxial ductile flow was the primary exhumation process. However, Behrmann

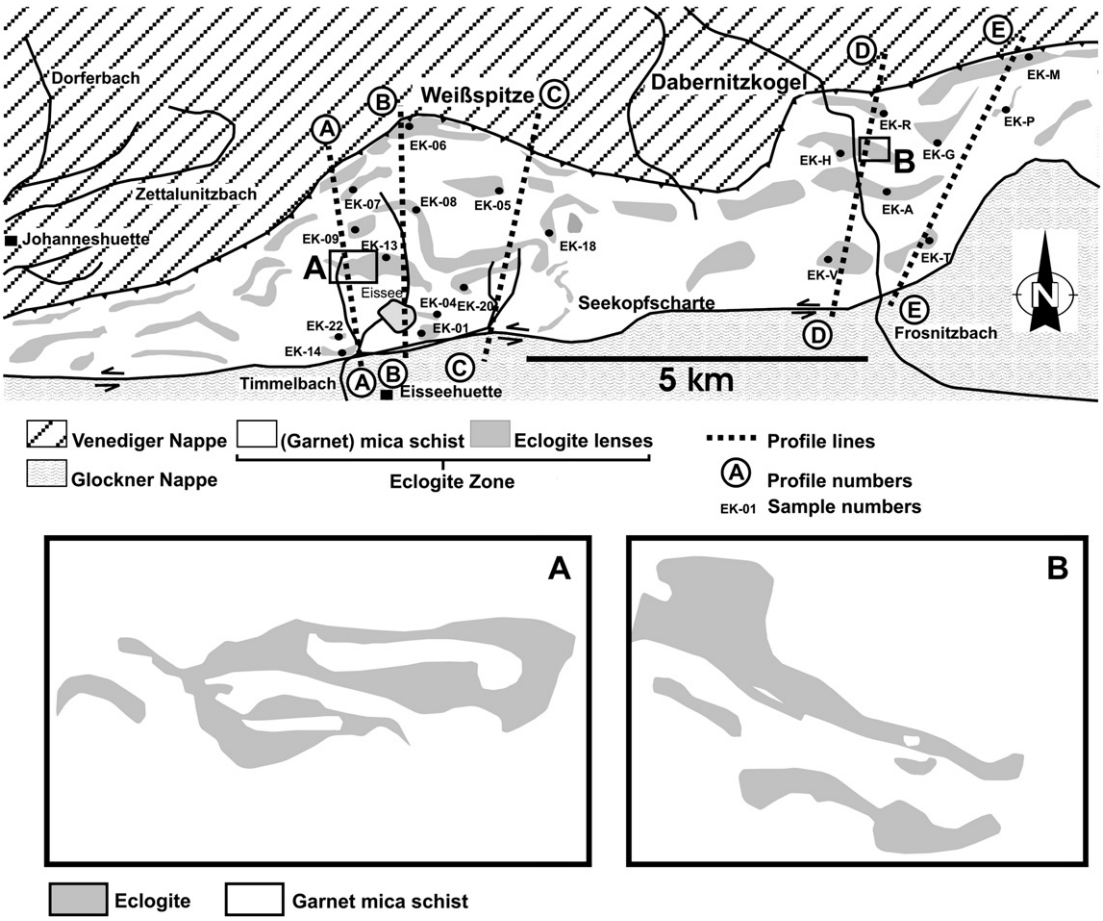

Fig. 2. Distribution of eclogite and surrounding metasediments in the Eclogite Zone and sample locations (black dots, with sample numbers). The sample profiles for LPO study are marked by dotted black lines and numbered A–E. Detailed mapped eclogite lenses are marked with black boxes and named as A & B.

and Ratschbacher (1989) did not consider that finite strain is a function of the instantaneous integrated strain along the exhumation path, which is a function of the depth dependence of the strain rate (Feehan and Brandon, 1999; Ring and Brandon, 1999). Therefore, vertical shortening in the deeply buried rocks of the Eclogite Zone is significantly higher than the amount of ductile thinning of the overburden. Behrmann and Ratschbacher (1989) questioned that buoyancy played an important role in driving the exhumation of the Eclogite Zone because the ratio of eclogite to matrix is too high. Raith et al. (1980) suggested that eclogites make up ~50% of the entire Eclogite Zone. Kurz and Froitzheim (2002) and Kurz et al. (1998, 2004) assumed wedge extrusion (Fig. 4) in a subduction channel, thereby postulating that the lower contact of the Eclogite Zone is a top-N thrust and the upper contact a top-S normal shear zone.

Kurz et al. (1998, 2004) divided the Tauern Window eclogites into two groups; a coarse grained variety and a fine grained, partly mylonitic variety. These authors distinguished two omphacite generations in the Eclogite Zone, omphacite-1 and omphacite-2, based on differences in grain size, grain shape and mineral chemistry and showed that omphacite-1 has a lower jadeite content (approx. 30 mol%) than omphacite-2 (approx. 50 mol%), thereby arguing that the two omphacite generations formed under different metamorphic conditions on the prograde path during eclogite formation during final underthrusting and accretion to the overriding plate.

While coarse grained eclogites mainly consist of omphacite-1, partly surrounded by omphacite-2, fine grained to mylonitic eclogites consist mainly of omphacite-2. Kurz et al. (1998, 2004) suggested that fine grained eclogites represent a stage of increased mylonitisation during peak metamorphism of the Eclogite Zone. Hoschek (2001), Kurz et al. (2004) and Glodny et al. (2005) showed that there is an increase in the jadeite content of omphacite-2 from core to rim and Hoschek (2007) showed that the rims formed at peak pressure of about 25 kbar.

3.2. Eclogite LPO

Previous studies (e.g. Helmstaedt et al., 1972; Godard and Van Roermund, 1995; Mauler, 2000; Bascou et al., 2001) showed that lattice preferred orientation of garnet typically displays randomly orientated patterns for eclogite, independent of metamorphic conditions or deformation processes. This is in agreement with a lack of LPO in garnet in this study (Fig. 5). The above cited studies concluded that omphacite is the main carrier of strain in eclogite.

Omphacite LPO have been investigated using universal stage techniques (e.g. Helmstaedt et al., 1972; Boundy et al., 1992; Godard and Van Roermund, 1995; Abalos, 1997) and recently using the rapidly improving electron backscatterred diffraction (EBSD) technique (e.g. Mauler, 2000; Mauler et al., 2001; Bascou et al., 2001; Piepenbreier and Stöckhert, 2001). The suitability of EBSD for studying omphacite LPO was demonstrated in detail by Mauler (2000) on natural and synthetic omphacites.

LPO in omphacite was first described by Helmstaedt et al. (1972), who divided omphacite textures into L-type LPO (linear fabrics) and S-type LPO (planar fabrics) (Fig. 6). L-type textures are characterized by strong point maxima at [001] near the lineation and a girdle distribution at [010] perpendicular to the lineation. S-type LPO is defined by the [001] axes lying in the foliation plane and

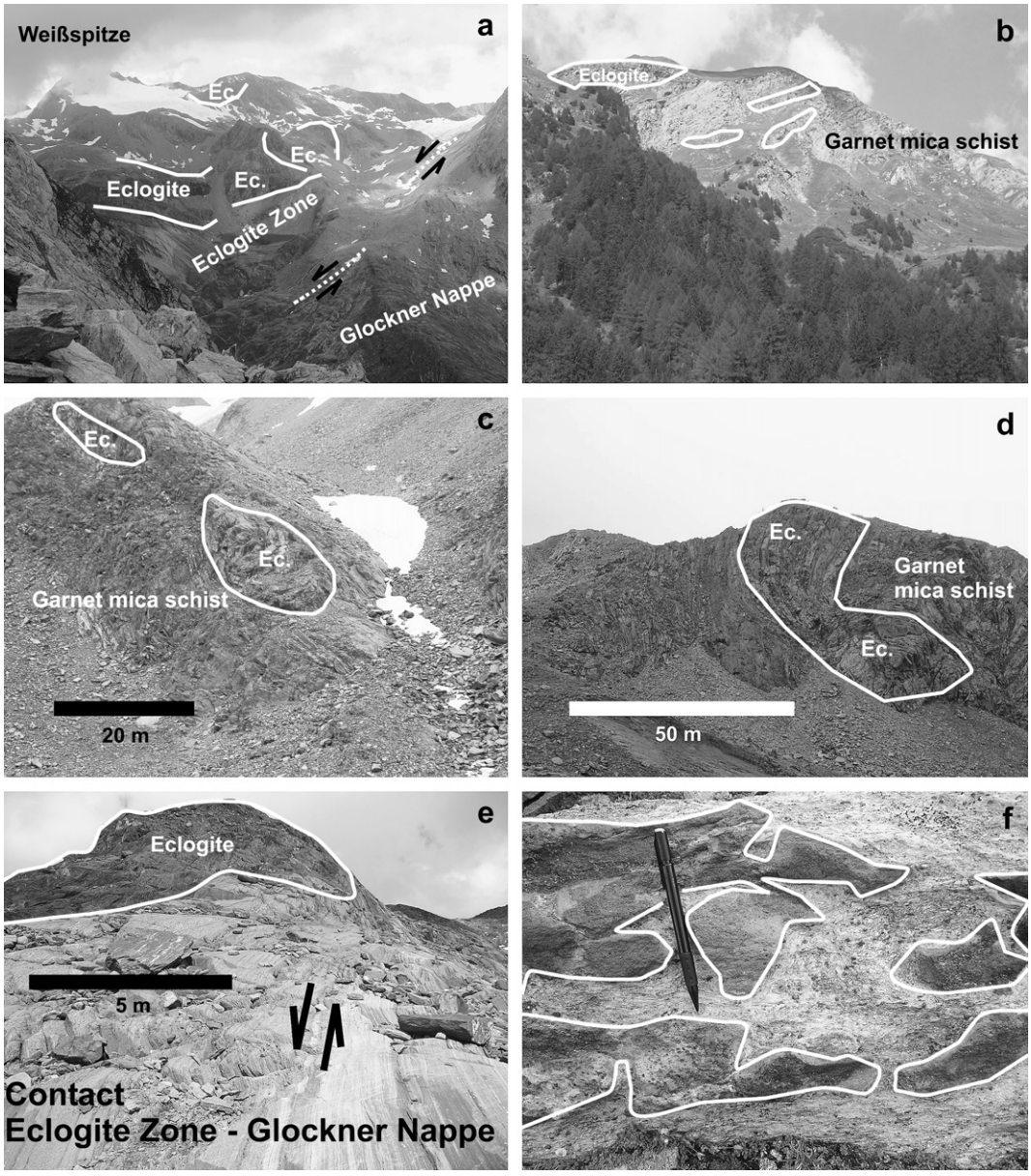

Fig. 3. (a) Overview of the central part of the Eclogite Zone, including marked eclogite lenses; (b, c, d) pictures of eclogite lenses (marked with white lines), embedded in garnet mica schist; (e) eclogite lense (marked with white lines) close to the contact shear zone at the top the Eclogite Zone; (f) detailed look at an eclogite lense, including small eclogite lenses (dark grey, marked with white lines) embedded in garnet mica schist (light grey).

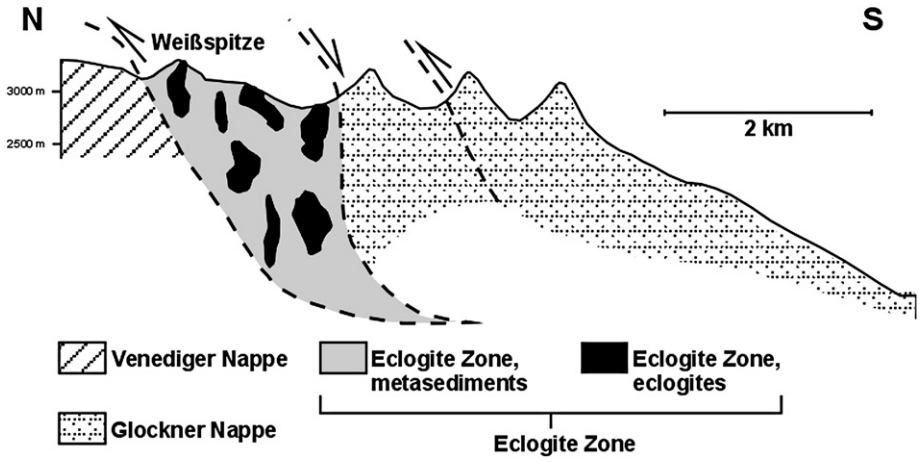

Fig. 4. Schematic cross section across the study area (central part of the Eclogite Zone), modified after Kurz et al. (1998).

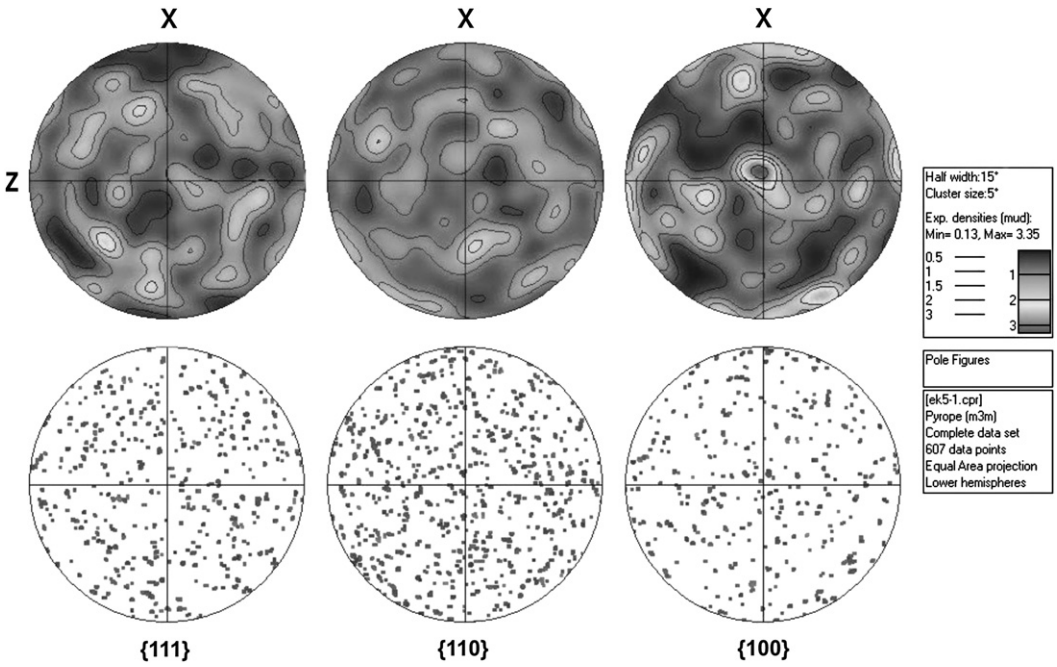

Fig. 5. Garnet LPO in eclogite sample EK-05 (Fig. 2) from the Eclogite Zone. (a) Contoured and (b) scattered diagram of the same sample. Lineation (X-direction) is vertical, Y is in the centre and Z is horizontal. Pole figures are plotted in equal area, lower hemisphere projection.

(010) planes parallel to the foliation. Godard and Van Roermund (1995) also recognized those two LPO end member types and described detailed transition fabrics between the end members. Helmstaedt et al. (1972) and Godard and Van Roermund (1995) argued that LPO development is related to shape preferred orientation (SPO) of omphacite and that a change in the LPO patterns reflects a changing deformation regime. L-type LPO is interpreted to result from deformation with constrictional strain, while S-type LPO results from a flattening strain type (Godard and Van Roermund, 1995; Abalos, 1997). Bouchez et al. (1983), Mainprice and Nicholas (1989), Boundy et al. (1992) and Abalos (1997) showed that non-coaxial deformation results in an obliquity between LPO and the principal strain axes ($X > Y > Z$), resulting in an asymmetric omphacite LPO pattern.

Bascou et al. (2001, 2002) studied omphacite LPO in eclogites developed under different metamorphic conditions from a number of orogens and compared the LPO patterns to the numerical LPO simulations of Molinari et al. (1987) and Lebenssohn and Tomé (1993). The latter two studies simulated the development of omphacite LPO patterns in different deformation regimes. The numerical results indicate a strong relationship between deformation mechanism and omphacite LPO and corroborated previous suggestions that flattening strain produces S-type LPO and constrictional strain L-type LPO, and also that non-coaxial deformation leads to asymmetric LPO patterns (e.g. Helmstaedt et al., 1972; Godard and Van Roermund, 1995; Abalos, 1997; Mauler, 2000). Bascou et al. (2001, 2002) subdivided omphacite LPO in patterns generated by simple shear, pure shear, axial compression, transpression and transtension. The results are summarized in Fig. 7 and are as follows: (a) Simulations of simple shear deformation produced patterns close to L-type LPO end members with asymmetric fabrics (Fig. 7a). (b) LPO patterns generated by pure shear depict transitional patterns between S- and L-type LPO. There is no asymmetry in the pure shear LPO (Fig. 7b). (c) Simulations of transtension generated LPO patterns similar to those resulting from simple shear, but the patterns have a stronger

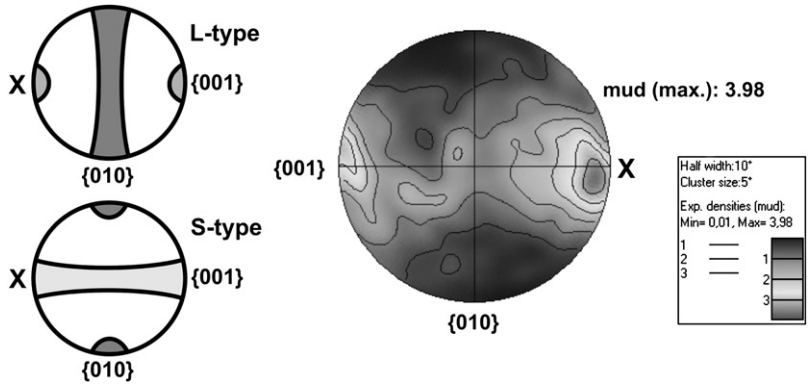

Fig. 6. Comparison between the omphacite LPO end members after Helmstaedt et al. (1972) and omphacite LPO of an eclogite from the Tauern Window (sample EK-9). Lineation (X – direction) is horizontal, Y in the centre and Z is vertical. The measured texture is close to the S-type end member. Light-grey – linear fabrics, dark grey – planar fabrics. Abbreviation: mud (max.) is mean unit deviation (maximum).

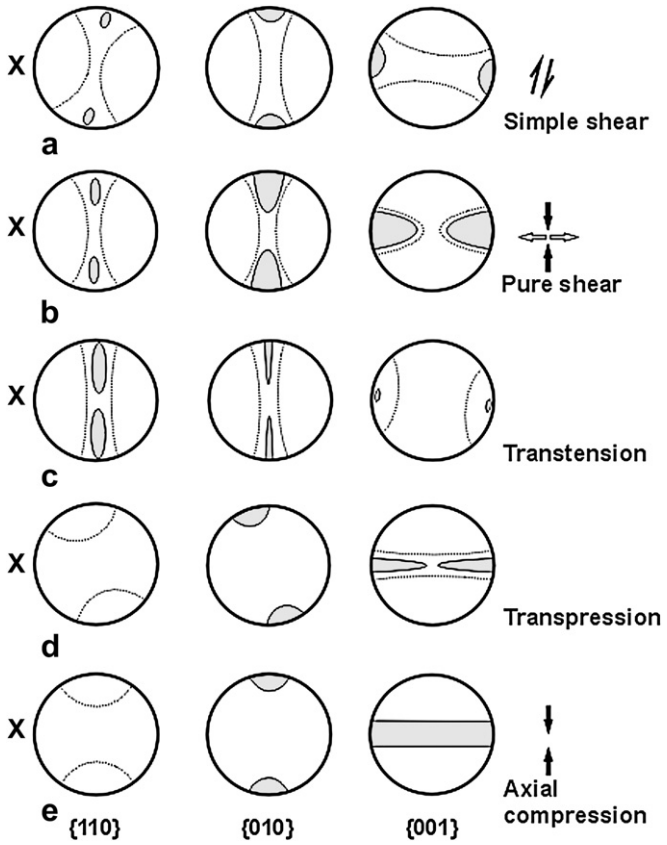

Fig. 7. Omphacite LPO generated under different deformation regimes (Bascou et al., 2001, 2002). Simple shear and transtension produce strong point maxima very close to the maximum extension direction X (X > Y > Z, principal strain axes) and also show asymmetric fabrics. Axial compression and transpression lead to S-type patterns and pure shear depicts a transitional fabric between S- and L-type LPO. Grey colour – strong signal (mean unit deviation maximum), dotted lines – weak signal.

asymmetry (Fig. 7c), the degree of which depends on the orientation of the shear plane and the shear direction. (d) Simulations of axial compression and transpression show largely similar, S-type patterns for both deformation regimes. Transpression patterns depict a less clear girdle distribution within the lineation at {001} than textures generated by axial compression (Fig. 7d,e). Transpression generated a slight obliquity at {010}, depending on the orientation of the shear plane and shear direction.

Kurz et al. (2004) argued, by studying combined petrologic and textural data from different (ultra) high pressure zones in the Alps, that S-type LPO is related to underplating and L-type LPO is related to exhumation. Kurz et al. (2004) reported lattice preferred orientation LPO data from 10 omphacite-bearing samples of the Eclogite Zone obtained from neutron diffraction analysis. Kurz et al. (2004) argued that omphacite-1 shows an S-type LPO pattern and displays flattening strain whereas omphacite-2 depicts an L-type LPO pattern resulting from constrictional strain. They further argued that the S-type fabrics are related to the prograde path while L-type fabrics are related to exhumation closely following the metamorphic peak. In other words, Kurz et al. (2004) interpreted the two different LPO patterns to reflect a change from subduction/accretion to exhumation.

Because Kurz et al. (1998, 2003) and Kurz and Froitzheim (2002) argued that the Eclogite Zone forms an extrusion wedge, and because at least some of the omphacite LPO fabrics are assumed to be related to the exhumation of the Eclogite Zone, one might expect that a systematic omphacite LPO study across the entire Eclogite Zone should result in a systematic change the sense of asymmetry of omphacite LPO fabrics. Assuming that non-coaxial deformation results in asymmetric LPO patterns (Bouchez et al., 1983; Mainprice and Nicholas, 1989; Boundy et al., 1992; Abalos, 1997), high strain areas, especially close to the boundaries between Eclogite Zone and its surrounding rock units, should lead to asymmetric LPO patterns, which should record different senses of asymmetry at the lower and upper contact of the Eclogite Zone. In this paper we set out to test this hypothesis.

4. Structural data

In general, structural data indicate a top-NNW shear sense for the lower and central parts of the Eclogite Zone, including sinistral components in the lowermost part of the unit, as well as sinistral shear sense in the uppermost part of the Eclogite Zone.

The footwall contact of the Eclogite Zone with the underlying Venediger Nappe is characterized by carbonate-rich and metapelitic mylonites (Fig. 8). The mylonitic foliation dips moderately to steeply to the S and contains a variably oriented stretching lineation with most lineations trending about NNW (Figs. 9 and 10). Kinematic indicators like shear bands and rotated clasts yielded a consistent top-NNW shear sense, which is best seen at the road to the Johannishütte in the Dorfertal. However, close to these top-NNW structures at the footwall contact of the Eclogite Zone mylonites with WSW–ENE-trending lineations recording a sinistral shear sense occur as well. Glodny et al. (in press) dated two carbonate-rich metapelitic mylonites showing top-N and sinistral shear sense. The sample showing top-NNW shear yielded a Rb–Sr age of 30.6 ± 0.9 Ma. Glodny et al. (in press) showed that Sr distribution among different white mica grain size fractions indicates that deformation of these mylonites occurred during decreasing pressures and temperatures (i.e. during exhumation) ceasing at greenschist facies conditions. Isotopic data suggest that sinistral shear lasted until 29.1 ± 0.5 Ma in the dated metapelitic mylonite. In this context it is important to note that the deformation ages date the last pervasive recrystallization, i.e., the end of ductile deformation (Freeman et al., 1997).

Granitic and pelitic gneisses in the directly underlying Venediger Nappe are commonly strongly deformed, display a platy fabric and a penetrative moderately to steeply S-dipping foliation on which a SW-plunging stretching lineation is developed (Fig. 10). Kinematic indicators also yield a top-NE sense of shear.

In the central part of the Eclogite Zone the deformation is of variable intensity. Carbonaceous, quartzitic and metapelitic rocks are commonly mylonitically deformed. The mylonitic structures have the same orientations as those at the footwall contact to the Venediger Nappe.

The hanging wall contact of the Eclogite Zone with the overlying Glockner Nappe is characterized by blueschist to greenschist facies carbonate-bearing, metapelitic and quartzitic mylonites. The mylonitic foliation is commonly steeply dipping to the S and contains a WSW–ESE-trending stretching lineation. The majority of the measured stretching lineations plunges at ~15–20° to the WSW but ENE-plunging lineations occur as well. Kinematic indicators in the mylonites record a sinistral shear sense (Figs. 8–10). Eclogite lenses close to the boundary are strongly deformed and elongated in the WSW–ENE-oriented shear direction.

The kinematic indicators from the non-eclogite rocks in general record blueschist- and greenschist-facies metamorphic conditions showing that they largely formed during exhumation. Glodny et al. (in press) showed that they started to form at 31.4 ± 0.4 Ma. The youngest age for this deformation event has been dated at 29.1 ± 0.5 Ma (Glodny et al., in press). Eclogite-facies metamorphism in the Eclogite Zone has been dated at 31.5 ± 0.7 Ma (Glodny et al., 2005) and thus at about the same time as the top-NNW and sinistral structures started to form.

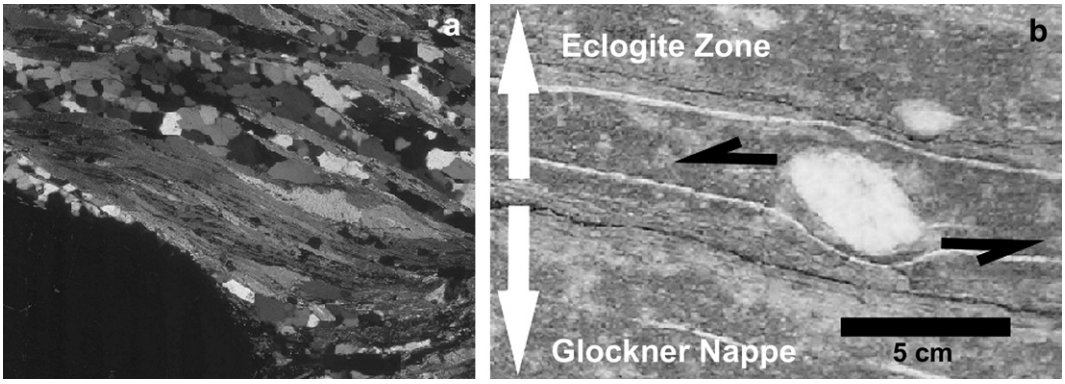

Fig. 8. (a) Carbonaceous mylonite (thin section, crossed nicols) marking the boundary between the Eclogite Zone and the underlying Venediger Nappe. (b) Marble mylonite at the boundary between the Eclogite Zone and the overlying Glockner Nappe. The asymmetric clast indicates a sinistral shear sense.

5. Analytical procedures

Omphacite lattice preferred orientation patterns of 20 eclogite samples from the Eclogite Zone were investigated using the electron backscattered diffraction (EBSD) technique (e.g. Prior et al., 1999) installed on two scanning electron microscopes (SEM). EBSD analyses were performed on a LEO 1530 SEM at Bayerisches Geoinstitut, Universität Bayreuth, and at Institut für Geowissenschaften, Universität Bochum. EBSD is based on the analysis of crystallographic diffraction patterns generated by an electron beam applied to a sample that is tilted at high (65–75°) angle from the horizontal plane within the vacuum chamber. The sample surface is highly polished with a colloidal silica suspension and lightly carbon coated. The mineral specific diffraction patterns (similar to Kikuchi patterns in a transmission electron microscope) were recorded on a phosphorus screen and indexed with CHANNEL 5 software by HKL technology.

The measurements on each sample were carried out in largely monomineralic areas. The stepsize varied between 50 and 150 μm, including measured areas of 0.5 – 1 cm^2. The numbers of indexed measured points, ranged from ~800 to ~25,000, depending on the microscope used, the grain size and the omphacite content of the measured areas. To ensure that both applied SEM instruments in this study produced comparable results, some samples were investigated with both microscopes. The indexed patterns are identical from both instruments.

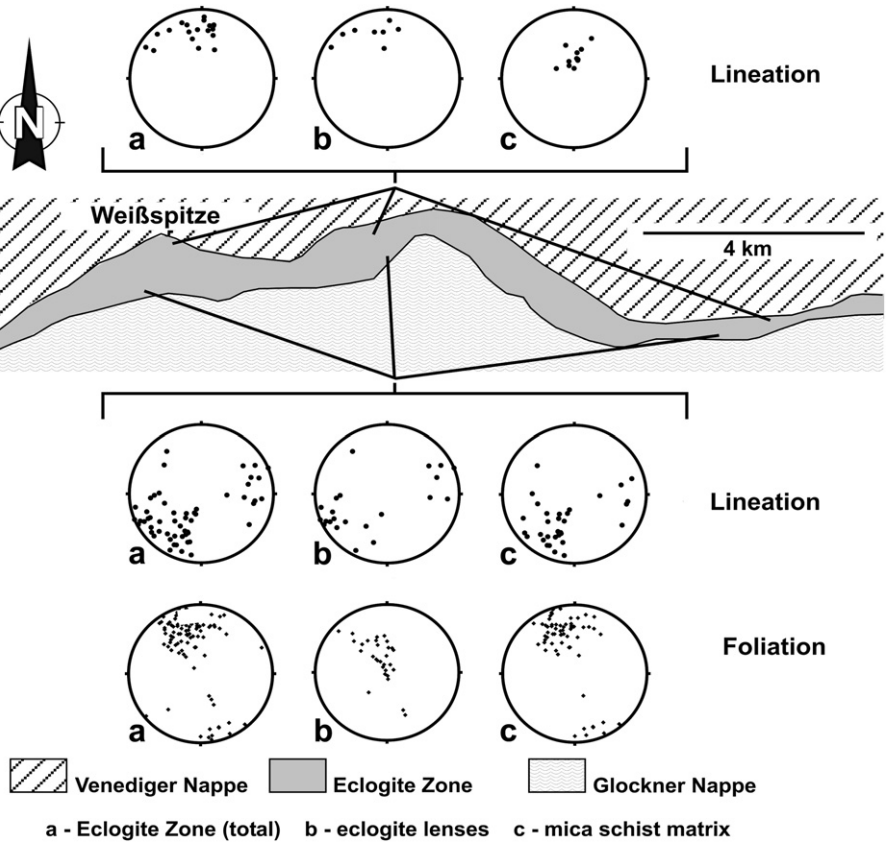

Fig. 9. Lineations (L) and poles to foliation (F) from the boundaries of the Eclogite Zone and its under- and overlying nappes. While the orientation of the lineation differs between lower and upper part from top-NNW to WSW–ENE, the strike of the foliation is orientated in SSE–NNW direction across the whole unit.

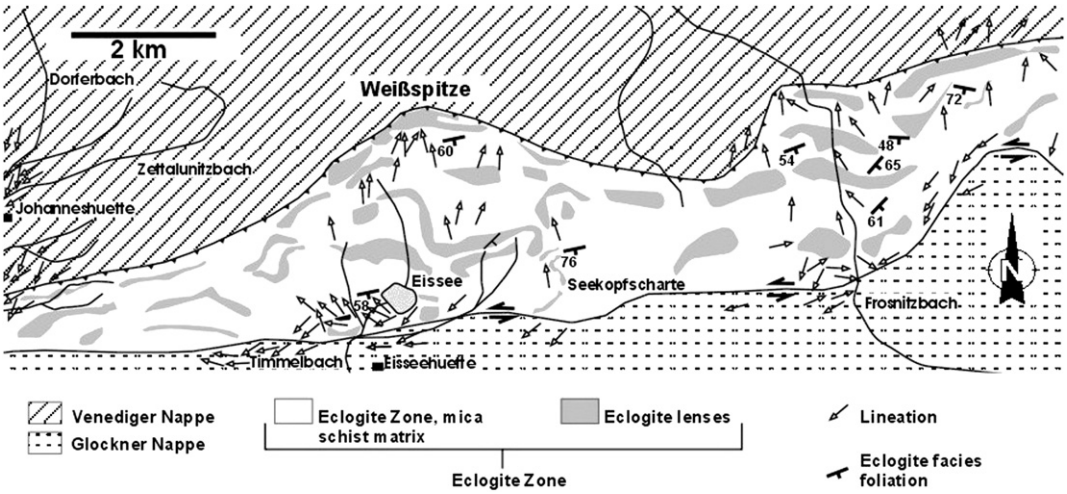

Fig. 10. Structural data of the central part of the Eclogite Zone. Stretching lineations are shown by black arrows with arrow heads pointing down-plunge. The lower boundary and most of the Eclogite Zone are characterized by NNW–SSE-trending lineations, whereas the boundary of the Eclogite Zone with the Glockner Nappe is characterized by WSW–ENE-trending lineations.

The samples were collected along five profiles across the Eclogite Zone. Each profile contains four samples. The measured omphacite LPO for each sample are plotted as polefigures in equal area and lower hemisphere projections.

6. Sample description

The studied eclogites can be divided into two types (E1 & E2, Fig. 11). This is in agreement with observations by Kurz et al. (2004). E1 eclogites represent a fine grained to mylonitic eclogite variety that is characterized by garnet layers embedded in a very fine grained omphacite groundmass. E1 eclogites (Figs. 11a and 12) are intensely foliated and commonly show a well-developed stretching lineation, which is parallel to the stretching lineation in the surrounding mica schists (see Section 4). E1 eclogites are much more common in the Eclogite Zone than E2 eclogites and fine grained to mylonitic E1 eclogites represent 17 out of 20 of the analyzed samples. The coarse grained E2 eclogites are randomly distributed in the Eclogite Zone and are not concentrated or lacking in distinct zones such as the boundaries of the Eclogite Zone.

The grain size of the garnets differs between fine grained eclogites. The majority of the E1 eclogites are characterized by garnets with a diameter of ~0.5–1 mm. These garnets are weakly elongated. On the other hand, the size of the garnets in E1 eclogites is between 3 and 5 mm and the garnets are euhedral. All garnets are concentrated in foliation-parallel layers.

The omphacite matrix in E1 eclogites is characterized by grain sizes up to 500 μm but commonly omphacite grain size is distinctly smaller. The grains are strongly lineated (Fig. 13c,d) in the penetrative foliation. No subgrain formation is observed. Mineral composition of omphacite and the microstructures in E1 eclogites do not show large variations and are very similar from sample to sample. Based on grain size and jadeite content, omphacite in E1 eclogites is omphacite-2 of Kurz et al. (2004). These authors argued that the mylonitic deformation of E1 eclogite occurred near and just after the metamorphic maximum and that the LPO patterns should yield an exhumation-related L-type fabric.

E2 eclogites (Figs. 11b–13b) are the coarse grained and distinctly less deformed eclogite variety. E2 eclogite has a semi-penetrative foliation but usually lacks a stretching lineation. No obvious shape preferred orientation of omphacite and garnet is visible in thin sections (Fig. 12c,d and 13a,b). The omphacite groundmass in E2 eclogites is characterized by larger grain sizes than in E1 eclogites. A grain size of 1–2 mm is very common, grains up to a size of 5 mm also occur. These omphacites represent the omphacite-1 generation of Kurz et al. (2004). Omphacite-1 only occurs in coarse grained eclogites. The omphacite grains are mainly randomly orientated and show pronounced subgrain formation (Fig. 13a,b) without any shape preferred orientation (SPO). Larger omphacite grains are optically zoned. In some samples, large omphacite-1 grains are surrounded by fine grained omphacite-2.

Beside garnet and omphacite, the mineral assemblages in both eclogite varieties include phengite, paragonite, kyanite, quartz, carbonate and opaques.

7. LPO patterns of omphacite

7.1. Description of LPO fabrics

The investigated LPO patterns from the Eclogite Zone are plotted as contoured polefigures in lower hemisphere equal area projections.

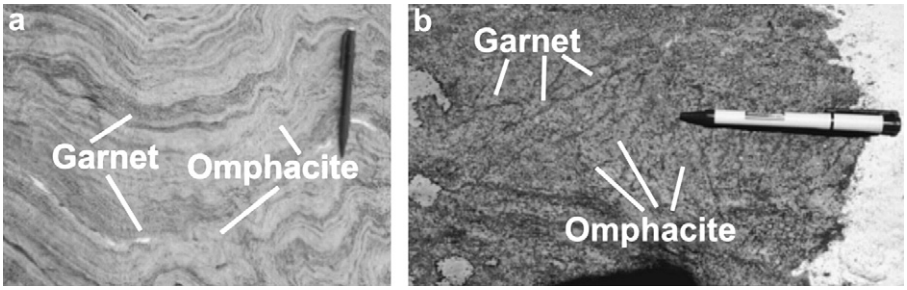

Fig. 11. (a) Fine grained E1 eclogite. (b) Coarse grained E2 eclogite.

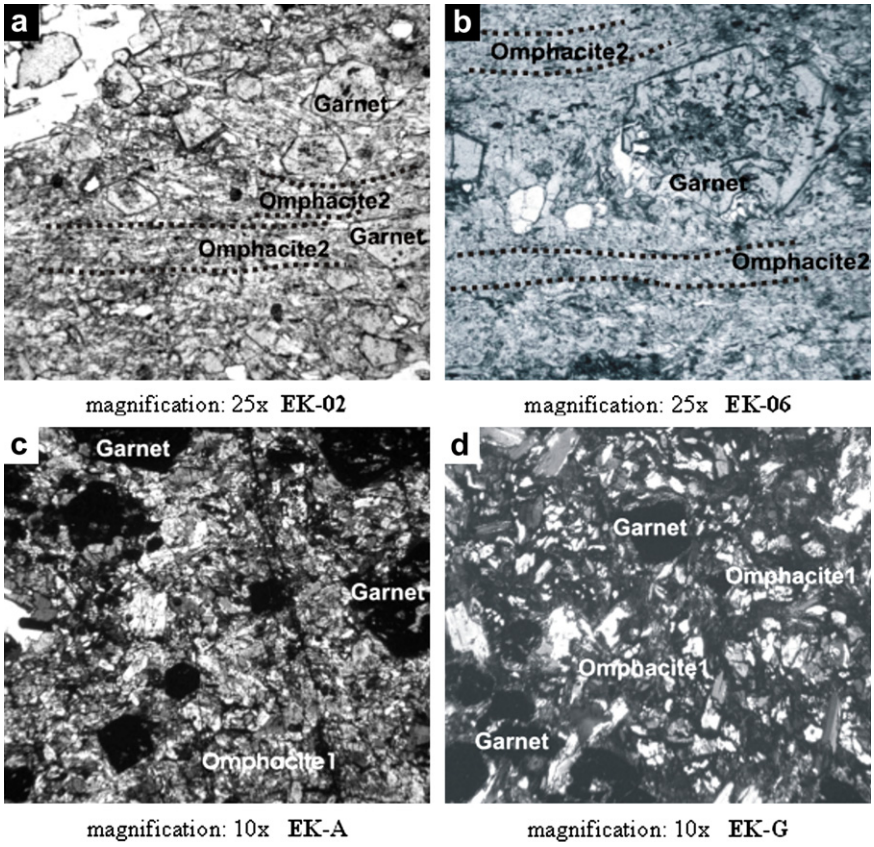

Fig. 12. Microphotographs of Tauern Window eclogites (all photographs are from XZ sections). (a, b) Fine grained E1 eclogites, foliation made up by omphacite alignment is marked by the dotted lines. (c, d) Coarse grained E2 eclogites, note lack of obvious foliation, crossed nicols.

Profiles A–E are arranged from west (profile A) to east (profile E) (Fig. 2).

Overall, the lattice preferred orientation patterns of omphacite from the Eclogite Zone (Fig. 14a–e) mainly show point maxima of {001} close to the lineation and are characterized by an alignment of {110} within the foliation plane. In most of the samples across the entire Eclogite Zone, the fabrics are symmetric, even close to the boundaries between Eclogite Zone and the surrounding tectonic units.

In the westernmost profile A (samples EK-07, EK-09, EK-22, EK-14, Fig. 14a), sample EK-09 contains coarse grained omphacite-1, all other samples contain fine grained omphacite-2. Sample EK-07 shows a symmetric transition pattern that resembles an S-type end member. Its LPO pattern was expected to display a significant asymmetry, but it is distributed very homogeneously in relation to lineation and foliation. Further to the top of the profile, sample EK-09 depicts an asymmetry, which is especially obvious for {001}. Sample EK-22 differs in comparison to all other samples from the entire Eclogite Zone by showing a LPO pattern that most closely resembles an L-type pattern. The uppermost sample EK-14, close to the overlying Glockner Nappe, is characterized by a symmetric transition pattern. There is no sign of any pronounced asymmetry close to the upper boundary of the Eclogite Zone.

In profile B (samples EK-06, EK-08, EK-13, EK-01, Fig. 14b), all samples contain fine grained omphacite-2. Overall, the LPO pattern of the four samples of profile B is more heterogeneous than those from profile A. The lowermost sample EK-06 shows a symmetric S-type pattern. This sample is from the basal shear zone that accomplished the emplacement of the Eclogite Zone onto the Venediger Nappe. However, there is no sign of any asymmetric omphacite lattice preferred orientation. Further to the top, sample EK-08 depicts only a weak mean unit deviation maximum (1.89). This sample fits in its symmetry with other samples, but its LPO is more randomly distributed than in most other samples. Sample EK-13 displays a S-type pattern. It also reflects a slight {001} asymmetry ($\sim 10^{\circ}$) in its girdle distribution in relation to the mesoscopic stretching lineation. In the uppermost part of profile B, sample EK-01 depicts a weak and not well developed pattern.

In profile C (EK-05, EK-18, EK-20, EK-04, Fig. 14c) all four samples contain fine grained omphacite-2. Sample EK-05 has the most strongly developed LPO that is a very symmetric S-type LPO. Close to lower and upper boundary of the Eclogite Zone, no obliquities are observed. In the structurally middle parts of profile C, omphacite LPO patterns do not show a distinct pattern. In particular sample EK-20 displays a near-random LPO with a weak maximum mean unit deviation. The uppermost sample EK-04 depicts a symmetric but weak pattern.

In profile D (samples EK-R, EK-H, EK-A, EK-V, Fig. 14d), sample EK-A contains coarse grained omphacite-1, all other samples are composed of fine grained omphacite-2. All samples from profile D depict symmetric LPO distributions close to the S-type end member. Sample EK-H from the central part of the profile has a much weaker LPO in comparison to the other samples.

In the easternmost profile E (samples EK-M, EK-P, EK-G, EK-T, Fig. 14e), sample EK-G is made up by coarse grained omphacite-1. All other samples contain fine grained omphacite-2. The LPO patterns of these four samples are similar to the ones from profile D in that the preferred orientation patterns are highly symmetric. An exception is the lowermost sample EK-M with a weakly developed LPO pattern. All other LPO patterns resemble S-type patterns very closely.

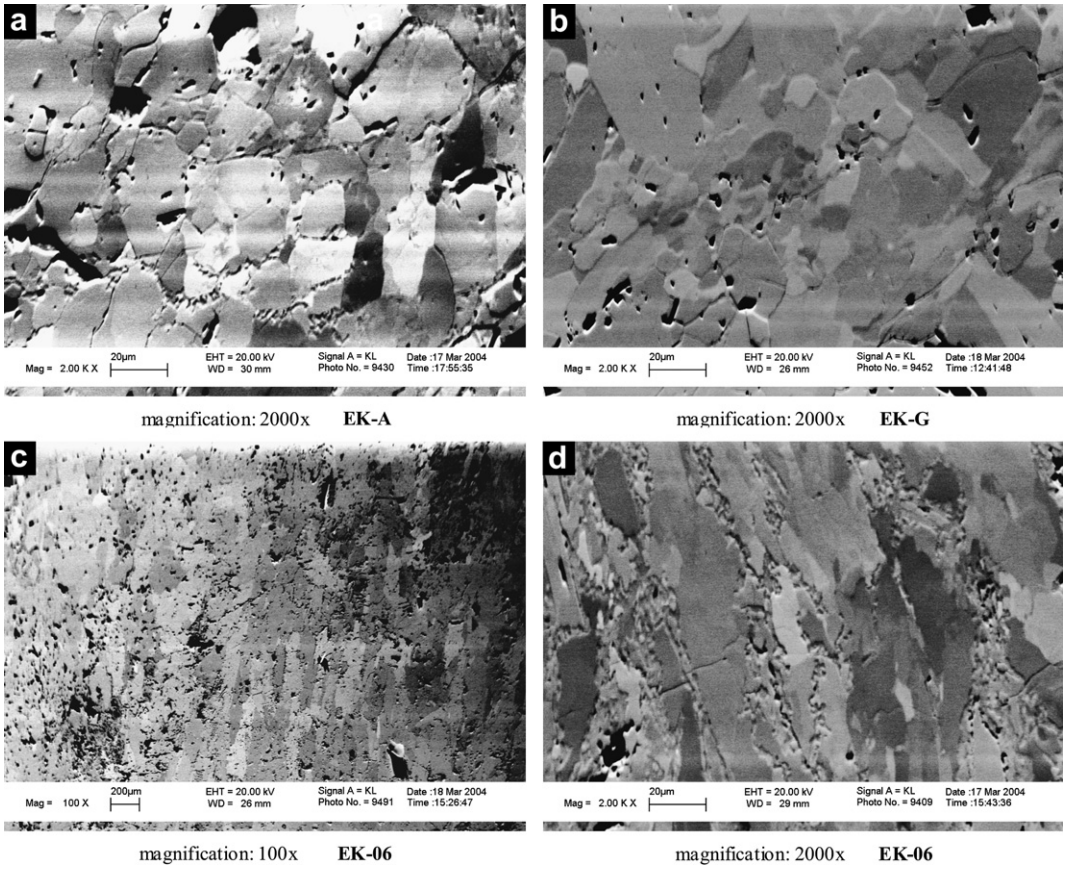

Fig. 13. Orientation contrast pictures of omphacite from XZ sections. (a, b) Subgrain development in omphacite-1 from coarse grained E2 eclogite. (c, d) Strongly aligned elongated omphacite-2 in fine grained E1 eclogite.

7.2. Interpretation

Based on the model of Helmstaedt et al. (1972), (Fig. 6), the 20 samples analysed in this study can be divided into three groups. The largest group contains 11 samples that are interpreted to reflect S-type LPO (EK-04, EK-05, EK-06, EK-07, EK-09, EK-13, EK-A, EK-P, EK-R, EK-T, EK-V). Six samples reflect transitional patterns (EK-01, EK-08, EK-14, EK-20, EK-M, EK-G) and one sample (EK-22) shows a L-type LPO pattern. Samples EK-18 and EK-H do not display a distinct LPO distribution. The majority of the samples have symmetric LPO patterns. The asymmetric patterns are also close to S-type textures.

In general, the LPO fabrics are homogeneous and do not show any significant changes, neither from west to east nor along N–S profiles across the Eclogite Zone. The only sample reflecting a strong L-type texture (EK-22) is from the central part of the Eclogite Zone and is not connected to either the lower or the upper boundary of the unit. Only a few samples reflect significant asymmetries but the asymmetries have no systematic pattern across the Eclogite Zone. Samples collected from the bounding shear zones of the Eclogite Zone (e.g. EK-06, EK-01, EK-M) depict symmetric LPO pattern that do not differ from the patterns in other samples.

More importantly, we do not find any significant difference in omphacite LPO associated with the two eclogite types. Coarse grained eclogites (E2, samples EK-09, EK-A, EK-G, Fig. 14) show S-type and transition patterns that do not differ from the LPO distributions in fine grained E1 eclogites. Omphacite-1, which is common in coarse grained eclogites, shows mainly identical patterns to omphacite-2, which is predominant in the fine grained samples.

8. Finite strain

Because the omphacite LPO patterns are, at least in part, related to finite strain, we carried out finite-strain analyses in augen gneiss from the Venediger Nappe directly below the Eclogite Zone. To quantify finite strain, the Fry method (Fry, 1979) was applied. The Fry method provides a graphic solution to the centre-to-centre method. The basic principle of the latter is that the distances between the centres of objects are systematically related to the orientation of the finite-strain ellipsoid.

Two-dimensional strain measurements were made on XY, XZ and YZ sections in order to estimate the three-dimensional strain geometry. A least-squares best-fit ellipse was calculated for each marker outline as well as its relative position and orientation. For Fry analysis, the central points of more than 100 feldspar grains per section were used to calculate strain. The strain estimates were used to calculate the finite-strain ellipsoid according to the modified least-square technique of Owens (1984).

All 10 analyzed samples plot in the oblate field of the Flinn diagram (Fig. 15). Axial ratios in XZ sections of the finite-strain ellipsoid range from 1.69 to 8.44. We have no control on possible volume changes during the accumulation of finite strain and cannot directly infer flattening strain type from the data. However, our data show pronounced oblate strain symmetry and a volume loss of >60% would be needed to shift the data into the field of constrictional strain. We consider such high volume strains unrealistic. Thus, we conclude that our strain data indicate flattening strain in the uppermost Venediger Nappe directly below the Eclogite Zone and we envisage that finite strain accumulated in the course of top-NNW thrusting of the Eclogite Zone onto the Venediger Nappe.

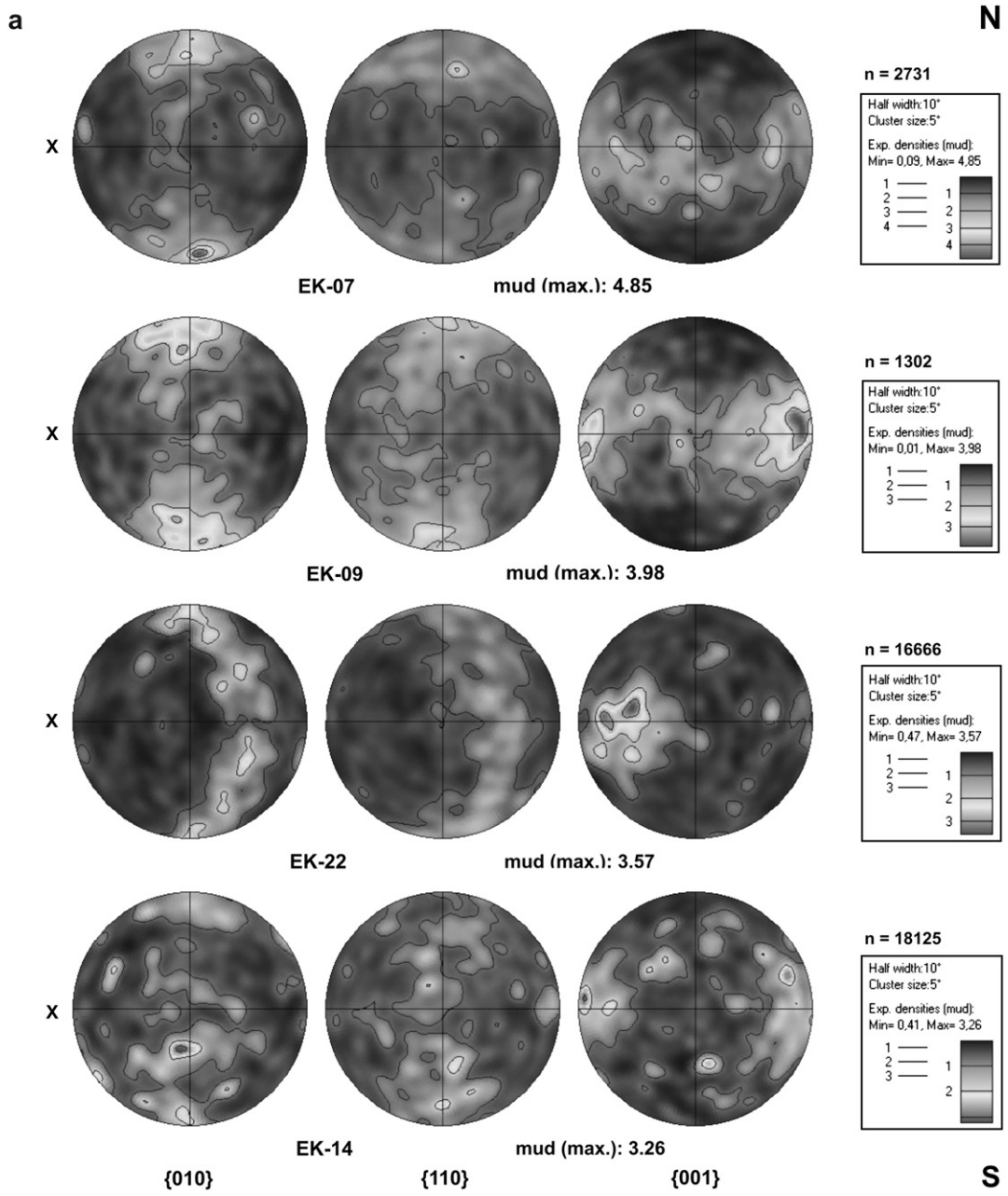

Fig. 14. (a) Omphacite LPO from samples of profile A. (b) Omphacite LPO from samples of profile B (legend and abbreviations as in (a)). (c) Omphacite LPO from samples of profile C (legend and abbreviations as in (a)). (d) Omphacite LPO from samples of profile D (legend and abbreviations as in (a)). (e) Omphacite LPO from samples of profile E (legend and abbreviations as in (a)). For sample and profile locations, see Fig. 2; pole figures are plotted in equal area, lower hemisphere projections; Lineation (X direction, marked on each pole figure) is horizontal, Y is at the centre and Z is vertical; abbreviations: mud (max) – mean unit deviation maximum; *n* – number of measure points. The lineation is orientated in top-N direction, except in the southernmost samples, where it is orientated in E–W direction.

9. Discussion

9.1. Comparisons with earlier work

Kurz et al. (1998) demonstrated that the Tauern Window eclogites represent two different eclogite types that formed under different metamorphic conditions during the prograde evolution and that the different eclogite types are characterized by different omphacite LPO patterns (Kurz et al., 2004). Overall, our omphacite LPO patterns do not show much variation and are close to S-type end members or transitional patterns tending towards S-type LPO textures. Furthermore, our omphacite LPO patterns show no differences between fine grained mylonitic E1 eclogite containing omphacite-2 and coarse grained E2 eclogites dominantly containing omphacite-1. Hence, our results contradict the results of Kurz et al. (1998, 2004) in that we did not manage to obtain systematically different omphacite LPOs for E1 and E2 eclogites. We maintain that our data set is distinctly greater than that of Kurz et al. (2004).

The transition from S-type to L-type presented in the relatively small dataset of Kurz et al. (2004) is indeed not very pronounced. We would argue that the omphacite-2 fabrics of Kurz et al. (2004) show a transition fabric. For example in samples WK526 and WK527 of Kurz et al. (2004) the girdle distribution of {001} is still recognizable and the {010} girdle is distinctly inhomogeneously distributed with a maximum in the S-type position. Furthermore,

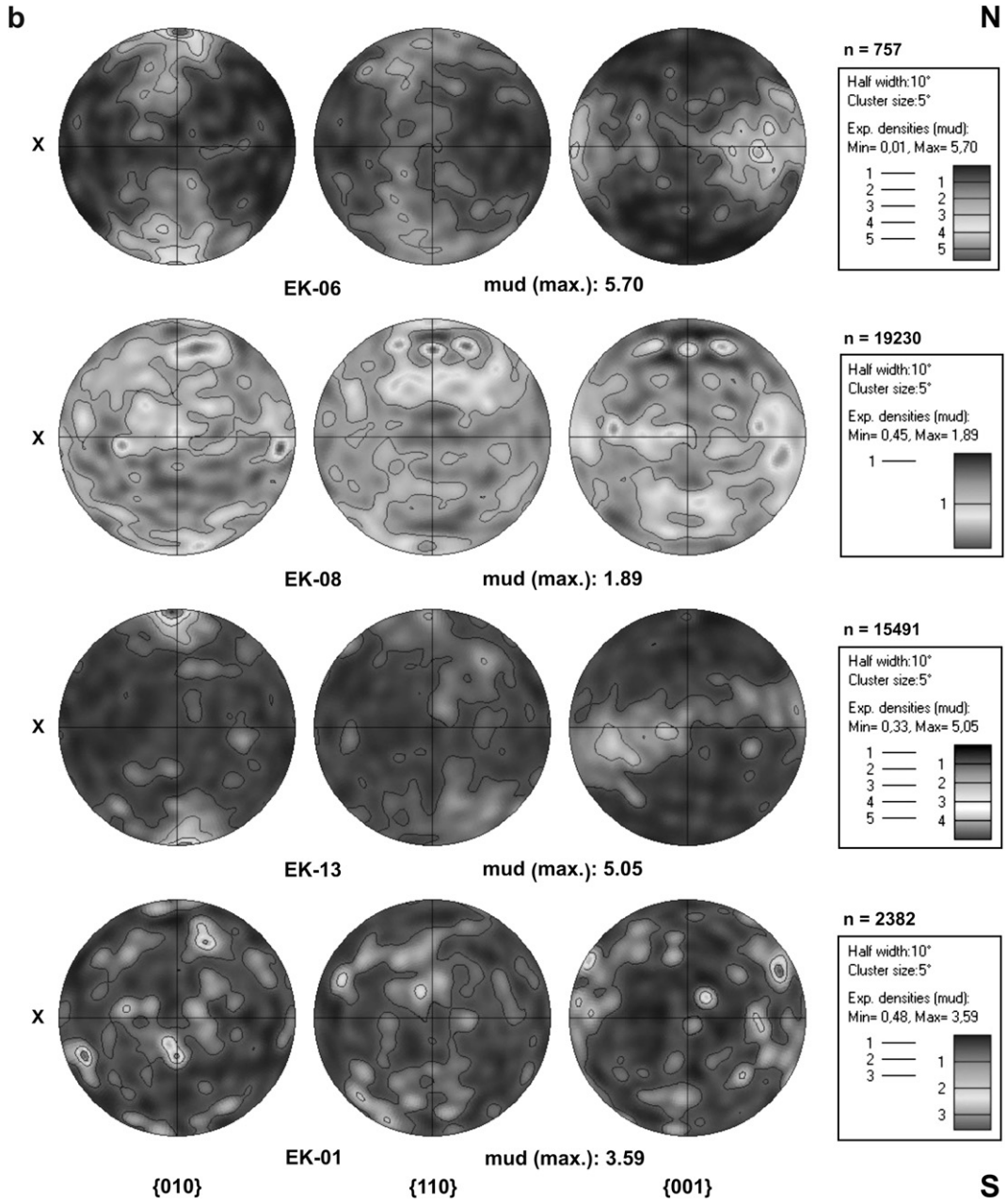

Fig. 14. (*continued*)

sample WK48–98 of Kurz et al. (2004), which has a transitional L-type omphacite-1 LPO fabric plots in the oblate field of the Flinn diagram. The L-type fabric in our sample EK-22 is much more distinct than in any of the samples analyzed by Kurz et al. (2004). In other words, the range of omphacite LPO patterns of Kurz et al. (2004) and our data set is largely comparable and does not differ significantly from each other. However, as argued above, the single L-type fabric recorded in EK-22 does not appear to have any general significance for omphacite LPO in the Eclogite Zone.

9.2. Regional implications of omphacite LPO fabrics

Given that the LPO patterns from both eclogite varieties do not differ and that omphacite-1 formed before and omphacite-2 near or at the metamorphic maximum (Kurz et al., 1998; Hoschek, 2007), we conclude that the S-type LPO patterns developed during underthrusting of the Eclogite Zone and accretion to the upper plate in the Oligocene at peak metamorphic conditions. It follows that our data argue that accretion occurred during coaxial deformation. Coaxial deformation, subvertical shortening and extension subparallel to the subduction thrust has been widely envisaged during underplating (Boundy et al., 1992; Stöckhert et al., 1997; Piepenbreier and Stöckhert, 2001; Ring and Brandon, 1999; Ring and Kassem, 2007).

The dominantly S-type omphacite LPO patterns fit with an overall transpressional deformation regime generally envisaged for the formation of the Tauern Window in the Oligocene (Rosenberg et al., 2004, 2007; Schmid et al., 2004). The S-type patterns are also in accord with flattening strain type in the Venediger Nappe directly below the Eclogite Zone. However, the transpressional regime has basically been inferred from the large-scale structures (i.e., nappe contacts and large-scale strike-slip shear zones) in the

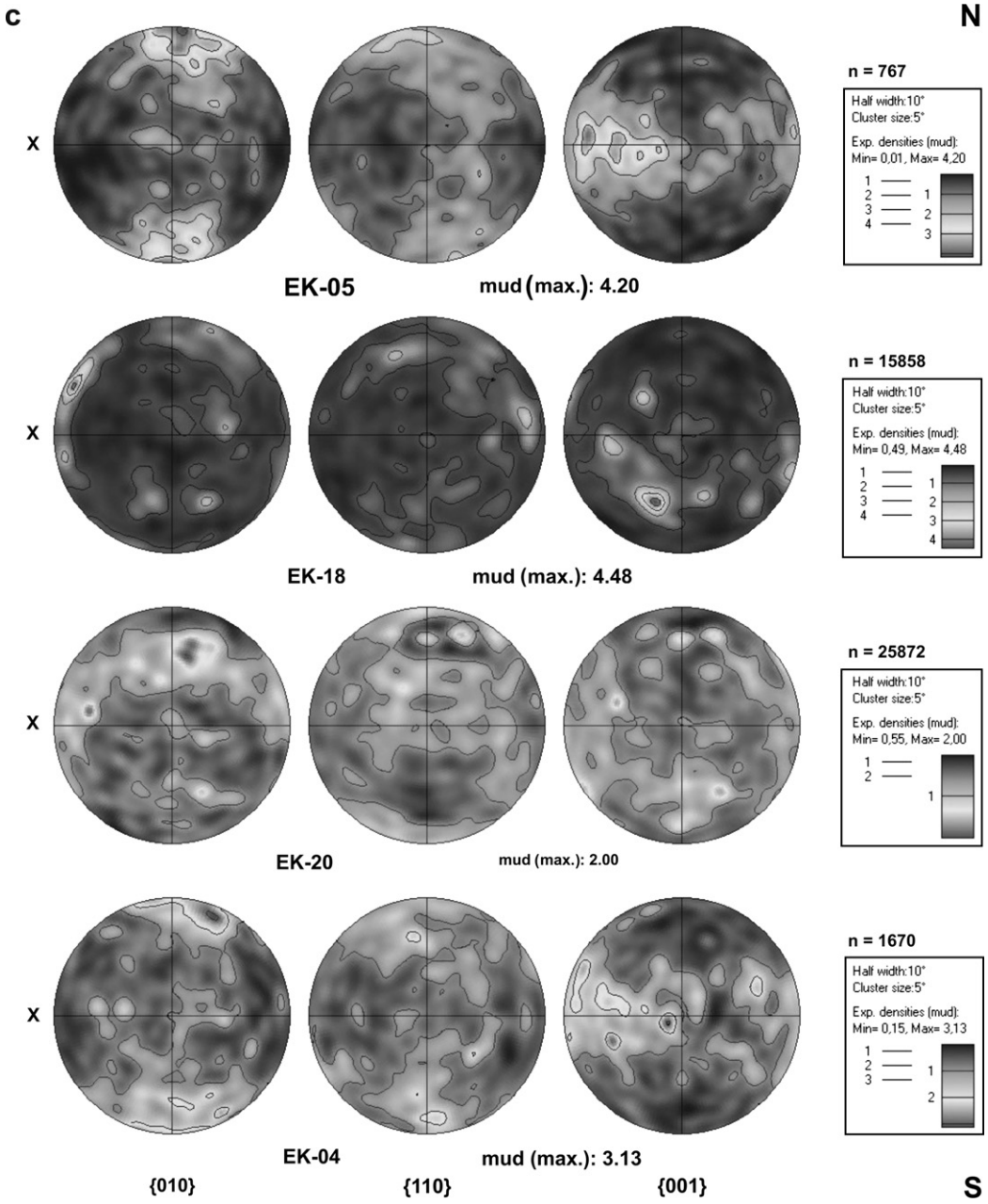

Fig. 14. (*continued*)

Tauern Window. All these structures mainly accomplished the exhumation of the Tauern Window. Likewise, the flattening finite strain from the uppermost Venediger Nappe has been attributed to the exhumation-related emplacement of the Eclogite Zone on top of the Venediger Nappe. Glodny et al. (2005) showed that subduction, prograde mineral reactions, eclogitization and subsequent exhumation of the Eclogite Zone proceeded rapidly. Therefore, we consider it most likely that the exhumation-related transpressional regime was already active during underthrusting and accretion of the Eclogite Zone.

Rapid exhumation of the Eclogite Zone (Glodny et al., 2005, in press) did not alter the omphacite LPO patterns in any significant way. The structures that reflect the geometry and kinematics of exhumation of the Eclogite Zone are recorded in the metasediments surrounding the eclogite blocks. These structures indicate top-NNW thrusting at the base and sinistral strike-slip shearing at the top of the Eclogite Zone. Sinistral shearing at the contact to the overlying Glockner Nappe rotated some of the eclogite boudins into an orientation parallel to the shear zone without modifying the omphacite fabrics to any degree. Such an interpretation is supported by the fact that eclogite samples from the shear zones that bound the Eclogite Zone have symmetric LPO patterns that are distinctly different from the dominantly asymmetric structures in the metasediments. No expected LPO asymmetries that correspond with different shear sense on both sides of the Eclogite Zone are reflected in the omphacite textures. We showed that the onset of the development of top-NNW and sinistral structures was coeval with the peak of eclogite-facies metamorphism. Furthermore, the structures continued to form during decreasing pressure and temperature until 29.1 $\pm$ 0.5 Ma (Glodny et al., in press). Therefore, the top-NNW and sinistral shear sense indicators characterize the kinematics of deformation of the entire exhumation processes from

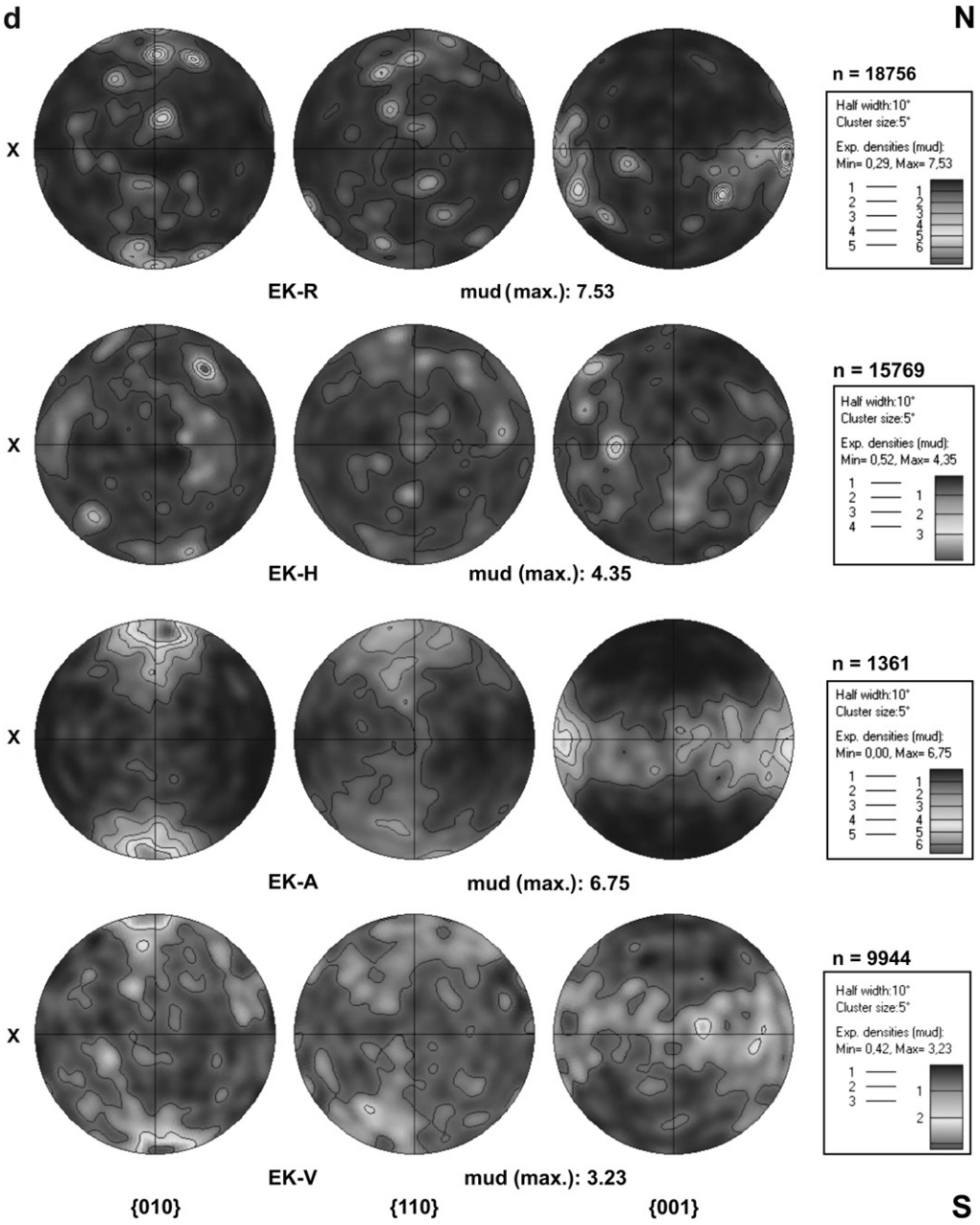

Fig. 14. (*continued*)

eclogite-facies conditions to depths were greenschist-facies metamorphism took place.

Given the transpressive character of the shear zone above the Eclogite Zone, the transport direction may have been steeper than the stretching lineation (Robin and Cruden, 1994). If so, the subhorizontal sinistral shear sense indicators would need to be reoriented into a steeper orientation for discussing the geometry during exhumation of the Eclogite Zone. Depending on whether this reorientation would be clockwise or anti-clockwise, an oblique or down-dip thrust-type or normal shear sense would result. We consider a normal shear sense more likely because it would have aided the extremely fast exhumation of the Eclogite Zone and would also readily explain the inverse metamorphic break between the Eclogite Zone and the Glockner Nappe. From that it can be inferred that the Eclogite Zone might indeed be an extrusion wedge as suggested by Kurz and Froitzheim (2002). However, we note that we do not have any data that would allow us to distinguish unequivocally between the thrust- and normal-type option.

9.3. Implications for fabric development in eclogites

We argued that the omphacite preferred orientation in the eclogites from the Eclogite Zone of the Alps record deformation processes before the eclogites have been exhumed. Data from eclogites of the Western Gneiss Region in Norway provide basically the same result (Neufeld, 2007). This is in agreement with Foreman et al. (2005), who also argued that omphacite textures in the Western Gneiss Region do not reflect the exhumation of this ultrahigh-pressure unit. We speculate that, at least in these two examples, the development of the omphacite LPO fabrics was strongly aided by the availability of fluids in the subduction channel. These fluids also facilitated the metamorphic reactions that

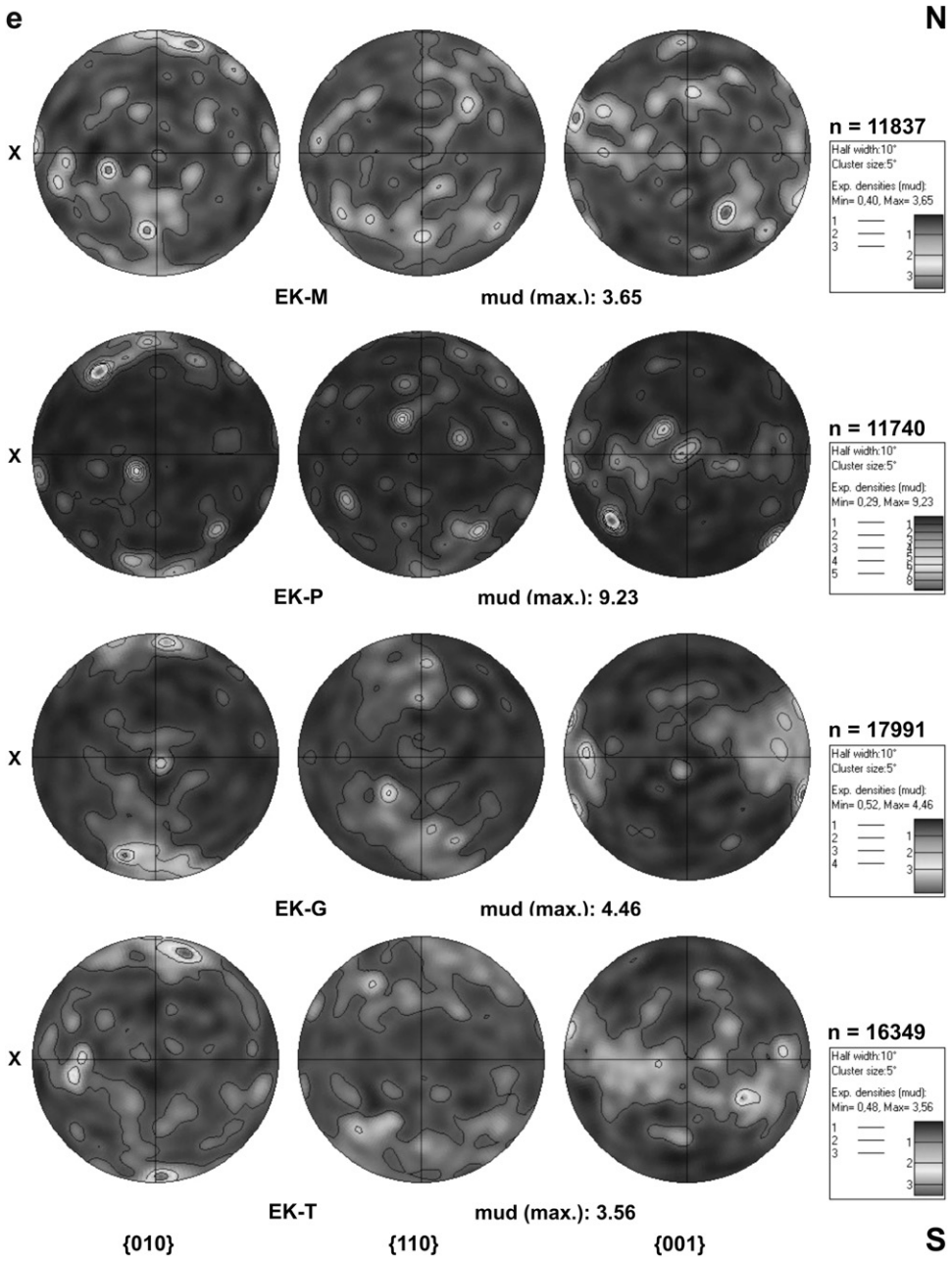

Fig. 14. (*continued*)

formed the eclogite-facies assemblages. For the Eclogite Zone, Hawkins et al. (2007) have shown that at prograde and peak high-pressure conditions a fully wetting aqueous fluid existed within the forming eclogites, and that most likely these fluids influenced the mode of strain accommodation and fabric development. Field evidence in West Norway indicates that zones of active eclogitization are easily deforming, an observation that can be explained by fluid presence and transformation plasticity (Austrheim et al., 1997). Whereas during subduction, accretion to the overriding plate under peak pressure fluids were present and facilitated deformation, it is known that shortly after onset of decompression, exhumation and cooling, fluids either migrate away or are consumed by incipient retrograde reactions, leaving an essentially 'dry' rock (Yardley, 1997; Yardley and Valley, 1997). It thus appears that in the moment of drying out, fabrics in the eclogite are frozen in. Later presence of fluids during exhumation would be evident from retrogression reactions. Retrogressed eclogites do occur within the Eclogite Zone, but have not been studied by us because of the abundant breakdown of omphacite during post-eclogitic overprint. In turn we conclude that the here studied eclogites remained devoid of free fluids after the end of eclogite-facies processes, and preserve their early underthrusting and accretion related fabrics from depth. This inference is in line with Glodny et al. (2005) who found fully preserved Sr-isotopic equilibria between the minerals of unretrogressed eclogites, equally indicating the absence of both crystal-plastic deformation and free fluids after peak-pressure eclogitization at 31.5 $\pm$ 0.7 Ma. Post-peak pressure deformation has been largely partitioned into the largely retrogressed, quartz-rich-metasediment dominated domains of the Eclogite Zone (Hawkins et al., 2007). The presence of these easily deforming metasediments is thus just another reason for preservation of peak-eclogite-facies fabrics within unretrogressed eclogites.

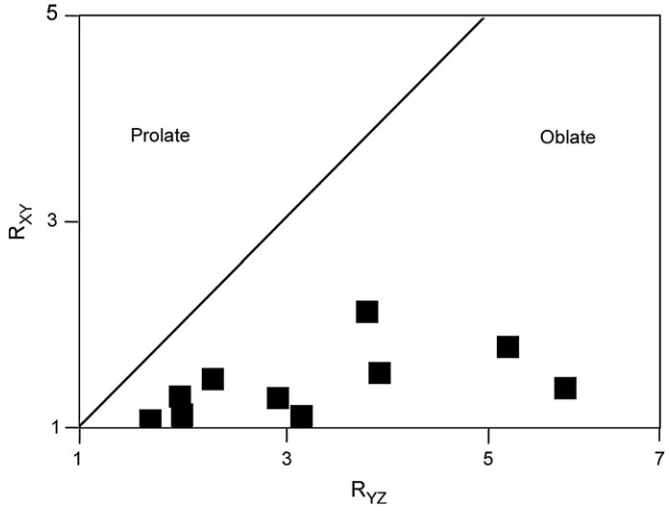

Fig. 15. Flinn diagram showing strain symmetry of finite strain derived from the application of the Fry method.

10. Conclusions

The study of the omphacite textures showed that the LPO patterns for the Eclogite Zone are not coupled with the kinematics of its surrounding metasediments. The omphacite LPO patterns from the eclogites of the Eclogite Zone developed during prograde metamorphism and most probably reflect coaxial accretion of the Eclogite Zone to the overriding Adriatic plate in the Oligocene. Exhumation related structures occur in the metasedimentary rock units that surround the eclogites. The strong partitioning of prograde structures in pristine eclogites and exhumation-related structures in metasediments is related to the availability of fluids during exhumation.

Acknowledgements

This study has been financially supported by Deutsche Forschungsgemeinschaft (grant Ri 538/23). We thank Johannes Glodny for discussions and Donna Whitney and Geoffrey E. Lloyd for constructive reviews that helped to improve the paper.

References

Abalos, B., 1997. Omphacite fabric variation in the Cabo Ortegal eclogite (NW Spain): relationship with strain symmetry during high-pressure deformation. Journal of Structural Geology 19, 621–637.

Austrheim, H., Erambert, M., Engvik, A., 1997. Processing of crust in the root of the Caledonian continental collision zone: the role of eclogitization. Tectonophysics 273, 129–153.

Bascou, J., Guilhem, B., Vaucez, A., Mainprice, D., Egydio-Silva, M., 2001. EBSD measured lattice preferred orientations and seismic properties of eclogites. Tectonophysics 342, 61–80.

Bascou, J., Tommasi, A., Mainprice, D., 2002. Plastic deformation and development of clinopyroxene lattice preferred orientations in eclogite. Journal of Structural Geology 24, 1357–1368.

Behrmann, J.H., Ratschbacher, L., 1989. Archimedes revisited. A structural test of eclogite emplacement models in the Austrian Alps. Terra Nova 1, 242–252.

Bouchez, T.M., Fountain, D.M., Lister, G., 1983. Fabric asymmetry and shear sense in movement zones. Geologische Rundschau 72, 401–419.

Boundy, T.M., Foutain, D.M., Austrheim, H., 1992. Structural development and petrofabrics of eclogite facies shear zones, Bergen Arcs, western Norway: implications for deep crustal deformational processes. Journal of Metamorphic Geology 10, 127–146.

England, P.C., Holland, T.J.B., 1979. Archimedes and the Tauern eclogites: the role of buoyancy in the preservation of exotic eclogite blocks. Earth and Planetary Science Letters 44, 287–294.

Feehan, J.G., Brandon, M.T., 1999. Contribution of ductile flow to exhumation of low-temperature, high-pressure metamorphic rocks: San Juan-Cascade nappes, NW Washington State. Journal of Geophysical Research 104, 10883–10902.

Foreman, R., Andersen, T.B., Wheeler, J., 2005. Eclogite-facies polyphase deformation of the Drøsdal eclogite, Western Gneiss Complex, Norway, and implications for exhumation. Tectonophysics 398, 1–32.

Frank, W., Höck, V., Miller, Ch., 1987. Metamorphic and tectonic history of the central Tauern Window. In: Flügel, H.W., Faupl, P. (Eds.), Geodynamics of the Eastern Alps. Deuticke, Wien, pp. 34–54.

Freeman, S.R., Butler, R.W.H., Cliff, R.A., Inger, S., Barnicoat, A.C., 1997. Deformation migration in an orogen-scale shear zone array: an example from the basal Briançonnais Thrust, internal Franco-Italian Alps. Geological Magazine 135, 349–367.

Fry, N., 1979. Random point distributions and strain measurements in rocks. Tectonophysics 60, 89–105.

Glodny, J., Ring, U., Kühn, A., Gleissner, P., Franz, G., 2005. Crystallization and very rapid exhumation of the youngest Alpine eclogites (Tauern Window, Eastern Alps) from Rb/Sr mineral assemblage analysis. Contributions to Mineralogy and Petrology 149, 699–712.

Glodny, J., Ring, U., Kühn, A. Coeval high-pressure metamorphism, thrusting, strike-slip, and extensional shearing in the Tauern Window, Eastern Alps. Tectonics, doi: 10.1029/2007TC002193, in press.

Godard, G., Van Roermund, H.L.M., 1995. Deformation-induced clinopyroxene from eclogites. Journal of Structural Geology 17, 1425–1443.

Hawkins, A.T., Selverstone, J., Brearley, A.J., Beane, R.J., Ketcham, R.A., Carlson, W.D., 2007. Origin and mechanical significance of honeycomb garnet in high pressure metasedimentary rocks from the Tauern Window, Eastern Alps. Journal of Metamorphic Geology 25, 565–583.

Helmstaedt, H., Anderson, O.L., Gavasci, A.T., 1972. Petrofabric studies of eclogite, spinel, websterite and spinel-lherzolite xenoliths from kimberlite-bearing breccia in pipes in southeastern Utah and northeastern Arizona. Journal of Geophysical Research 77, 4350–4365.

Holland, T.J.B., 1977. Structural and metamorphic studies of eclogites and associated rocks in the central Tauern region of the eastern Alps. DPhil thesis, Oxford University.

Hoschek, G., 2001. Thermobarometry of metasediments and metabasites from the Eclogite Zone of the Tauern Window, Eastern Alps, Austria. Lithos 59, 127–150.

Hoschek, G., 2007. Metamorphic peak conditions of eclogites in the Tauern Window, Eastern Alps, Austria: thermobarometry of the assemblage garnet + omphacite + phengite + quartz. Lithos 93, 1–16.

Kurz, W., Neubauer, F., Dachs, E., 1998. Eclogite meso- and microfabrics: implications for the burial and exhumation history of eclogites in the Tauern Window (Eastern Alps) from p-T-d paths. Tectonophysics 285, 183–209.

Kurz, W., Froitzheim, N., 2002. The exhumation of eclogite-facies metamorphic rocks – a review of models confronted with examples from the Alps. International Geology Review 44, 702–743.

Kurz, W., Fritz, H., Froitzheim, N., Tenzcer, V., Unzog, W., 2003. Mechanics of the exhumation of eclogite-facies metamorphic rocks in convergent plate margins: models and examples from the Alps. In: Geophysical Research Abstracts, Vol. 5. European Geophysical Society.

Kurz, W., Jansen, E., Hundenborn, R., Pleuger, J., Schäfer, W., Unzog, W., 2004. Microstructures and crystallographic preferred orientations of omphacite in alpine eclogites: implications for the exhumation of (ultra-) high-pressure units. Journal of Geodynamics 37, 1–55.

Lebenssohn, R.A., Tomé, C.N., 1993. A self-consistent anisotropic approach for the simulation of plastic deformation and texture development of polycrystals: application to zirconion alloys. Acta Metallurgica Materialia 41, 2611–2624.

Mainprice, D., Nicholas, A., 1989. Development of shape and lattice preferred orientations: applications to seismic anisotropy of the lower crust. Journal of Structural Geology 11, 175–189.

Mauler, A., 2000. Texture and microstructures in eclogites. Electron backscattered diffraction applied on samples from nature and experiment. PhD. Thesis, Eidgenössische Technische Hochschule, Zürich.

Mauler, A., Godard, G., Kunze, K., 2001. Crystallographic fabrics of omphacite, rutile and quartz in Vendee eclogites (Armorican Massif, France). Consequences for deformation mechanism and regimes. Tectonophysics 342, 81–112.

Molinari, A., Canarova, G.R., Azhy, S., 1987. A self-consistent approach of the large deformation polycrystal viscoplasticity. Acta Metallurgica 35, 2983–2994.

Neufeld, K., 2007. Lattice preferred orientation in omphacite: examples from the Tauern Window, Austria and the Western Gneiss Region, Norway. PhD thesis, Universität Mainz.

Owens, W.H., 1984. The calculation of a best-fit ellipsoid from elliptical sections on arbitrarily orientation planes. Journal of Structural Geology 6, 571–578.

Piepenbreier, D., Stöckhert, B., 2001. Plastic flow of omphacite in eclogites at temperatures below 500 °C – implications for interplate coupling in subduction zones. International Journal of Earth Sciences 90, 197–210.

Prior, D., Boyle, A.P., Brenker, F., Cheadle, M.C., Day, A., Lopez, G., Peruzzo, L., Potts, G.J., Reddy, S., Spiess, R., Timms, N.E., Trimby, P., Wheeler, J., Zetterström, L., 1999. The application of electron backscatter diffraction and orientation contrast imaging in the SEM to textural problems of rocks. American Mineralogist 84, 1741–1759.

Raith, M., Mehrens, Ch., Thöle, W., 1980. Gliederung, tektonischer Bau und metamorphe Entwicklung der penninischen Serien im südlichen Venediger-Gebiet. Osttiroler Jahrbuch der Geologie. Bundesanstalt 123, 1–37.

Ring, U., Brandon, M.T., 1999. Ductile strain, coaxial deformation and mass loss in the Franciscan complex: implications for exhumation processes in subduction zones. In: Ring, U., Brandon, M.-T., Lister, G.S., Willett, S. (Eds.), Exhumation Processes: Normal Faulting, Ductile Flow and Erosion. Special Publications Geological Society London, vol. 154, pp. 55–86.

Ring, U., Brandon, M.T., Willett, S., Lister, G.S., 1999. Exhumation processes. In: Ring, U., Brandon, M.T., Lister, G.S., Willett, S. (Eds.), Exhumation Processes:

Normal Faulting, Ductile Flow and Erosion. Special Publications Geological Society London, vol. 154, pp. 1–28.
Ring, U., Kassem, O.K.K., 2007. The nappe rule: why does it work? Journal Geological Society London 164, 1109–1112.
Ring, U., Ratschbacher, L., Frisch, W., 1988. Plate-boundary kinematics in the Alps: Motion in the Arosa suture zone. Geology 16, 696–698.
Robin, P.Y.F., Cruden, A.R., 1994. Strain and vorticity patterns in ideally ductile transpression zones. Journal of Structural Geology 16, 447–466.
Rosenberg, C.L., Brun, J.P., Gapais, D., 2004. Indentation model of the Eastern Alps and the origin of the Tauern Window. Geology 32, 997–1000.
Rosenberg, C.L., Brun, J.P., Cagnard, F., Gapais, D., 2007. Oblique indentation in the Eastern Alps: insights from laboratory experiments. Tectonics 26, TC2003, doi: 10.1029/2006TC001960.
Schmid, S.M., Fügenschuh, B., Kissling, E., Schuster, R., 2004. Tectonic map and overall architecture of the Alpine orogen. Eclogae geologicae Helveticae 97, 93–117.
Selverstone, J., 1988. Evidence for east-west crustal extension in the eastern Alps: implications for the unroofing history of the Tauern Window. Tectonics 7, 87–105.
Selverstone, J., 1993. Micro- to macro-scale interactions between deformation and metamorphism, Tauern Window, Eastern Alps. Schweizerische Mineralogische und Petrographische Mitteilungen 73, 229–239.
Stöckhert, B., Masonne, H.J., Nowlan, E.U., 1997. Low differential stress during high pressure metamorphism: the microstructural record of a metapelite from the Eclogite Zone, Tauern Window, Eastern Alps. Lithos 41, 103–118.
Yardley, B.W.D., 1997. The evolution of fluids through the metamorphic cycle. In: Jamtveit, B., Yardley, B.W.D. (Eds.), Fluid Flow and Transport in Rocks. Chapman & Hall, London, pp. 99–117.
Yardley, B.W.D., Valley, J.W., 1997. The petrologic case for a dry lower crust. Journal of Geophysical Research 102, 12173–12185.